AD-A150 646 THREE IMAGE EXPERTS WHICH HELP DISTINGUISH LUNG TUMORS 1/1
FROM NON-TUMORS(U) ROCHESTER UNIV NY DEPT OF COMPUTER
SCIENCE W LAMPETER FEB 84 TR-123 N00014-80-C-0197
UNCLASSIFIED F/G 6/5 NL

END
FILMED
DTIC

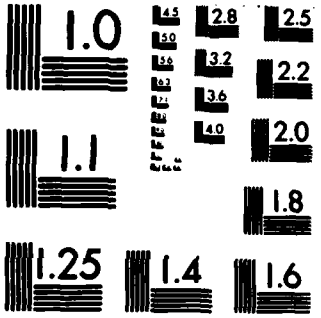

(2)

THREE IMAGE EXPERTS WHICH HELP DISTINGUISH LUNG TUMORS FROM NON-TUMORS

William Lampeter
Computer Science Department
University of Rochester
Rochester, NY 14627

TR 123
February 1984

rochester

Department of Computer Science
University of Rochester
Rochester, New York 14627

THREE IMAGE EXPERTS WHICH HELP DISTINGUISH LUNG TUMORS FROM NON-TUMORS

William Lampeter
Computer Science Department
University of Rochester
Rochester, NY 14627

TR 123
February 1984

The work reported herein was done in partial fulfillment of the requirements for a Master of Science degree in Photographic Science at the Rochester Institute of Technology.

I wish to thank the Computer Science Department of the University of Rochester for the kind use of their facilities and for the honor of having access to their faculty. All the research contained in this thesis and the preparation of this document were completed at the University of Rochester.

****

This work was funded in part by the following: Office of Naval Research Grant N00014-80-C-0197; Defense Advanced Research Projects Administration Grant N00014-82-K-0193; and National Institutes of Health Public Health Service Grant 5R01-HL21253-05.

SECURITY CLASSIFICATION OF THIS PAGE (When Data Entered)

REPORT DOCUMENTATION PAGE		READ INSTRUCTIONS BEFORE COMPLETING FORM
1. REPORT NUMBER TR 123	2. GOVT ACCESSION NO. A150646	3. RECIPIENT'S CATALOG NUMBER
4. TITLE (and Subtitle) Three Image Experts Which Help Distinguish Lung Tumors from Non-Tumors		5. TYPE OF REPORT & PERIOD COVERED Technical Report 6. PERFORMING ORG. REPORT NUMBER
7. AUTHOR(s) William Lampeter		8. CONTRACT OR GRANT NUMBER(s) N00014-80-C-0197 and N00014-82-K-0193
9. PERFORMING ORGANIZATION NAME AND ADDRESS Computer Science Department, University of Rochester, Rochester, NY 14627		10. PROGRAM ELEMENT, PROJECT, TASK AREA & WORK UNIT NUMBERS
11. CONTROLLING OFFICE NAME AND ADDRESS Defense Advanced Research Projects Agency 1400 Wilson Boulevard Arlington, VA 22209		12. REPORT DATE February 1984 13. NUMBER OF PAGES 9
14. MONITORING AGENCY NAME & ADDRESS(if different from Controlling Office) Office of Naval Research Information Systems Arlington, VA 22217		15. SECURITY CLASS. (of this report) Unclassified 15a. DECLASSIFICATION/DOWNGRADING SCHEDULE

16. DISTRIBUTION STATEMENT (of this Report)

Distribution of this document is unlimited.

17. DISTRIBUTION STATEMENT (of the abstract entered in Block 20, if different from Report)

18. SUPPLEMENTARY NOTES

None

19. KEY WORDS (Continue on reverse side if necessary and identify by block number)

Accession For
NTIS GRA&I ☒
DTIC TAB ☐
Unannounced ☐
Justification
By
Distribution/
Availability Codes
Dist | Avail and/or Special
A-1

20. ABSTRACT (Continue on reverse side if necessary and identify by block number)

The design of three vision-expert programs is described. The vision experts are based on appearance models of objects in a typical chest radiograph which were derived using information from human experts. Each expert is based on a different technical concept. The rib expert uses relational constraints on parameter (Hough transform) space to determine if a rib has been detected; the vascularity expert uses a back-projected Hough transform; and the nodule expert uses features which were derived from studies of the

DD FORM 1 JAN 73 1473 EDITION OF 1 NOV 65 IS OBSOLETE

SECURITY CLASSIFICATION OF THIS PAGE (When Data Entered)

nodule recognition process of radiologists. The efficacy of the descriptive models and their implementations are evaluated. The processes of development and implementation of image experts are discussed.

ABSTRACT

The design of three vision-expert programs is described. The vision experts are based on appearance models of objects in a typical chest radiograph which were derived using information from human experts. Each expert is based on a different technical concept. The rib expert uses relational constraints on parameter (Hough transform) space to determine if a rib has been detected; the vascularity expert uses a back-projected Hough transform; and the nodule expert uses features which were derived from studies of the nodule recognition process of radiologists. The efficacy of the descriptive models and their implementations are evaluated. The processes of development and implementation of image experts are discussed.

INTRODUCTION

The Automated Nodule Detection System (ANDS) is an experimental program for prescreening of chest radiographs for nodular abnormalities [Lampeter, 1983]. The results of ANDS are presented to a radiologist for final inspection/diagnosis. ANDS is based on the system described by Ballard and Sklansky [1973]. It differs essentially in the methods of: pre-processing (spline filtering), rib detection (a local technique is used) [Ballard, 1978], and the way in which false positives are rejected (the subject of this paper). The processes of ANDS are outlined in Fig. 1.

The candidate nodule detector in ANDS is based on a simple circle detector [Ballard and Sklansky, 1973]. This detector locates all approximately circular shapes which have a specified radius. Not all of these reported shapes, or candidate nodules (CNs), are in fact nodules. The goal of the experts is to distinguish the nodules from the non-nodules which are comprised of: vascular structures, points on or near the lung borders, ribs, nipples, and noise. Thus, these experts reduce the false positive rate and present the user with a display of sites in the film that are most similar to nodules. Fig. 2 illustrates a display of CNs before and after processing by the image experts.

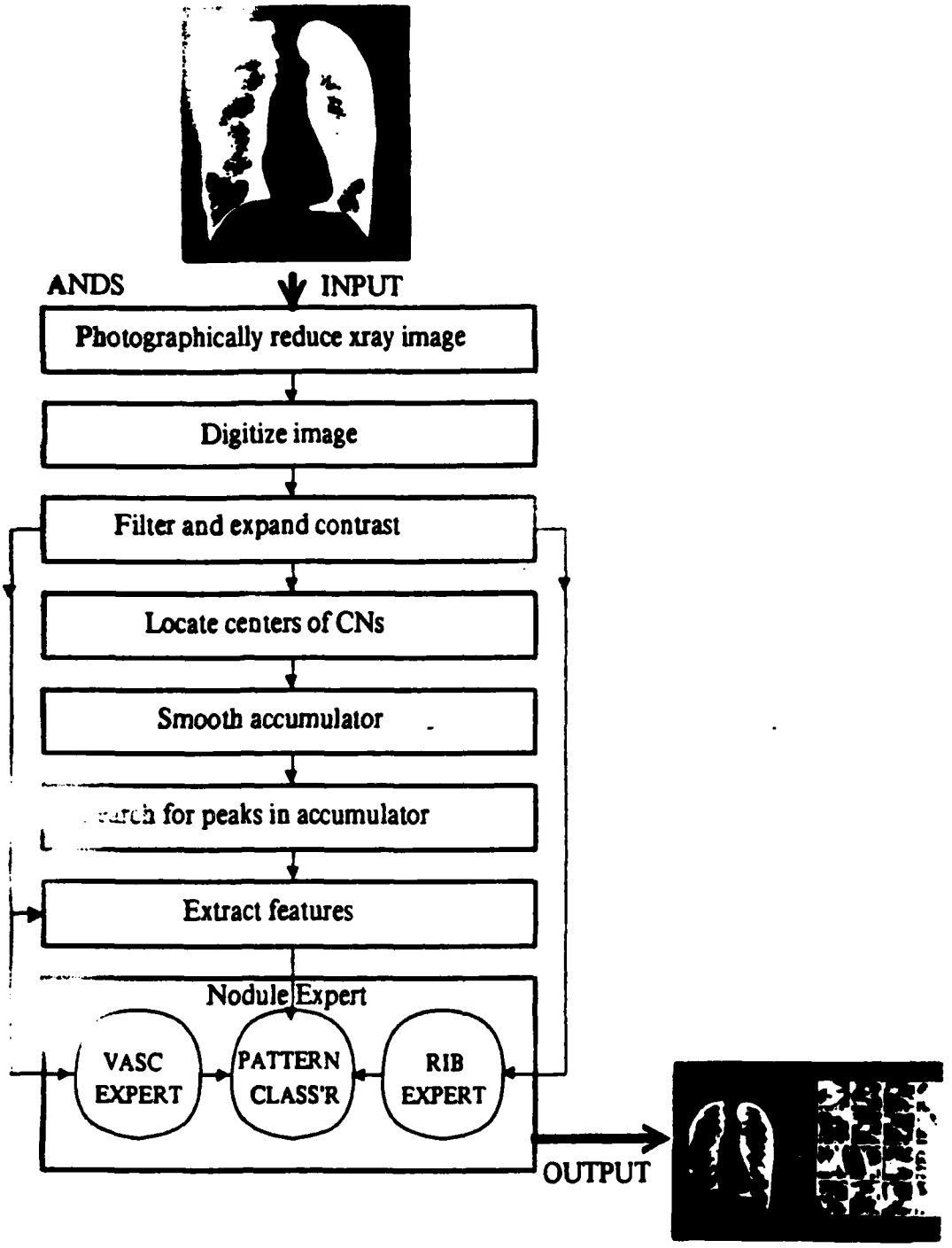

Figure 1. The Automated Nodule Detection System (ANDS). A chest radiograph is presented to ANDS which analyzes it for the presence of pulmonary nodules and which produces a display of candidate nodule sites. ANDS incorporates three vision experts: a Rib Expert and a Vascularity Expert provide information to a pattern classifier which classifies a CN; and a Nodule Expert uses a set of rules to distinguish nodules from false positives, causing the obvious false positives to be omitted from the CN sites that are presented to the radiologist.

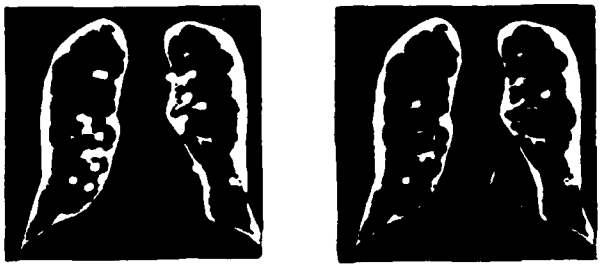

Figure 2. ANDS prescreens a chest radiograph, using image experts to reduce the number of CNs that a radiologist must inspect (right). The vascularity expert presumes that the CNs near the mediastinum arise because the underlying anatomic structure is straight. With enough imagination this may be seen in the image processed by ANDS without the image experts (left), where all CNs are displayed.

The experts are each derived from appearance models of the objects they detect. The rib appearance model is based on my interpretation of the appearance of a section of a rib which has been detected as a candidate nodule. The vascularity expert is based on the concept that vascular structures (bronchi *etcetera*) and their branches, which when imaged end-on appear as CNs, are somewhat striaght. The nodule expert uses features which were derived from psychophysical studies of the appearance characteristics which distinguish detected from undetected nodules. The success or failure of these experts depends on the accuracy of the models. I shall describe each expert and the technical approach it embodies.

THE IMAGE EXPERTS

Rib Expert - Relational Constraints in Parameter Space

The salient features of a rib, which lead to its detection as a possible nodule, are given in the appearance model. Relational constraints and the rib expert algorithm are derived from the appearance model. This model states the following properties:

- -- a rib is a relatively bright object bounded by two parallel edges;
- -- by convention, the rib edges are separated by 180 degrees;
- -- the width of the rib is approximately the diameter of the sought-after nodule;
- -- the rib edges are approximately centered around the CN;
- -- the parallel rib edges are the strongest (gradient magnitude) of all edges near the CN;
- -- these edges are also the most extensive in the (windowed - 64 x 64 pixels) image of a CN.

From these properties the relational constraints of a non-rib and a rib are derived. The parametric equation of a line [Duda and Hart, 1972] is used to map candidate rib edge-elements from image space to parameter space, $P[\rho, \Theta]$:

$$\rho = x\cos\Theta + y\sin\Theta \qquad \text{(Eq. 1)}$$

The angular orientation of the edge obtained by a Sobel edge operator is used to limit the range of Θ. In parameter space the following exclusive relations among location and values of peaks must exist before the detector responds that the parameterized object has been detected. An image is detected as a non-rib using the following relational constraints:

$$\exists\ \{(\rho_1,\Theta_1), (\rho_2,\Theta_2), \ldots, (\rho_n, \Theta_n)\} : P[\rho_1, \Theta_1] >= \beta MAX(P), \text{ and } P[\rho_2, \Theta_2] >= \beta MAX(P), \text{ and } P[\rho_n, \Theta_n] >= \beta MAX(P),$$

where: β is the rejection weight ($0 < \beta \leq 1$).

An image is detected as a rib using the following relational constraints:

$$\exists\ \{(\rho_1,\Theta_1), (\rho_2,\Theta_2)\} : 0 \leq |\rho_1 - r| < \epsilon, \text{ and } 0 \leq |\rho_2 - r| < \epsilon, \text{ and } 0 \leq |\Theta_1 - \Theta_2 - 180| < \eta, \text{ and } P[\rho_1,\Theta_1] \geq \alpha MAX(P), \text{ and } P[\rho_2,\Theta_2] \geq \alpha MAX(P).$$

where: ϵ and η are error tolerances on ρ and Θ, respectively; and α is a weight ($0 \leq \alpha < 1$) on the maximum in P.

The above criteria essentially state that: a non-rib has been detected if more than two peaks (in parameter space) have values greater than the rejection threshold; and a rib has been detected if only two peaks whose Θ values are about 180 degrees apart and have values above a specified threshold. The relational constraints are embodied in the following algorithm which operates on an image of a CN. Here, successively more (and weaker in magnitude) edges are included for testing using the relational constraints. At each iteration the relational constraints are tested; first, a test attempts to reject the image as that of a rib and another test attempts to accept it as an image of a rib. The output of the rib expert is used by the nodule expert.

```
BEGIN (* Rib Expert *)
    PctOfEdgesConsidered = 2;
    WHILE( PctOfEdgesConsidered .LE. SomeMaximumValue )
    BEGIN (* loop *)
        (* consider all edges whose gradient magnitudes are in the top PctOfEdgesConsidered
        of all gradient magnitudes *)
        IF( TestForNonRib() (* if most prominant edges are not relatively parallel *) )  BEGIN
            return NOT-RIB;
        END
        IF( TestForRib() (* if there are only two prominant and parallel edges *) )  BEGIN
            return RIB-DETECTED;
        END
        PctOfEdgesConsidered = PctOfEdgesConsidered + 2;
    END (* loop *)
    return NOT-SURE;
END (* Rib Expert *)
```

Performance of Rib Expert

The rib expert was tested on 2750 CNs whose classifications are known. Table 1 illustrates the known classifications of the 311 CNs that were detected by the rib expert.

Performance of Rib Expert on Entire Database

		Taught As:												
Rib Exp.	**% OK**	**ri**	**SR**	**sv**	**lv**	**SN**	**MN**	**LN**	**lb**	**mb**	**SB**	**NI**	**un**	**Count**
RIB	0.15	47	1	27	15	4	3	3	33	87	3	1	87	311

213 ribs were taught
311 CNs were classified as *rib* by the Rib Expert

Table 1. The distribution of CNs per classification (ri = rib; SR = nodule on rib; sv, lv = small and large vascularity, respectively; SN, MN, LN = small, medium, and large nodule, respectively; SB = nodule on border; NI = nipple; un = unclassified, that is, did not fit into any of the above classes) of the 311 CNs that were detected by the rib expert.

Note the rather large number of CNs along the lung borders (**lb** and **mb**) that were detected as ribs. This suggests a modification of the rib appearance model. Vertical edges (the lung borders) should be included in the relational constraints for a non-rib. Although 15% of the CNs that were detected by the rib expert were in fact

classified as ribs (true positives), 22% (47) of all CNs classified as ribs (213) were detected. When the output of the rib expert is combined with the nodule appearance features, which add information about ribbiness, computed by the feature extracter 54% (116) of all ribs are correctly identified (sensitivity). Overall, 62% (116/187) of all CNs classified as ribs by the nodule expert were in fact ribs.

A nodule that overlaps a rib may be detected as a rib by a global rib detector [Ballard, 1978] or by the rib expert described herein. The nodule expert augments the information about ribbiness provided by the rib expert with nodule appearance features which aid in distinguishing between a rib and a nodule on a rib. The combined use of the rib expert output and the nodule appearance features by the nodule expert resulted in the correct identification of 50% (7/14) of all CNs classified as *nodule on rib*. An additional 36% (5/14) of all CNs originally classified (taught) as *nodule on rib* were classified as *rib* by the nodule expert. Thus, 86% (12/14) of all CNs classified as *nodule on rib* were correctly detected as some sort of nodule.

Vascularity Expert - Back-projected Hough Transform

The appearance model for the vascularity expert is rather simple. It is based on the notion that vascularity originates near the mediastinum and that the structures that support or contain the vascularity are relatively straight. Thus, the expert tests CNs that are in a region near the mediastinum for colinearity. Each CN votes for a set of lines which may pass through it. This voting occurs in a space which defines, by Eq. 1, a set of parameterized lines. The number of votes at a peak is back-projected onto the locations of the CNs in image space that gave rise to that peak. Each point in P corresponds to a line. Points with the most votes (peaks in P space) correspond to lines that explain the most evidence. Thus, the vascularity expert computes a measure of colinearity of the CNs which are near the mediastinum. This weight is an input of the nodule expert.

Performance Evaluation

Table 2 summarizes the performance of the vascularity expert on 2750 CNs. The database contained 717 CNs that were classified as vascularity; 105 (15%) of these were detected as such.

Performance of Vascularity Expert on Entire Database

		Taught As:												
Vasc Exp.	% OK	ri	SR	sv	lv	SN	MN	LN	lb	mb	SB	NI	un	Count
VASC	0.46	16	0	73	32	0	0	1	0	71	0	0	35	228

717 vascular structures were taught
228 CNs were classified as *vascularity* by the Vascularity Expert

Table 2. The distribution of CNs per classification of the 228 CNs that were detected by the vascularity expert.

Nodule Expert - BMDP7M

Radiologists miss 25-30% of all nodules smaller than 1.0 cm [Garland, 1959; Yerushalmy, 1955]. Revesz *et. al.* [1977] studied the appearance characteristics that distinguish undetected from detected nodules. These features in addition to others (relative distance measures from the top of the lung and each vertical border, and the outputs from the experts) are computed and used by the nodule expert.

Twenty-three features are computed for each CN. BMDP7M [Dixon and Brown, 1979], a commercial statistical package for computing a linear discriminant function, was "trained" with 1911 23-element feature vectors whose classifications were specified. This package was used to determine which features are required for discriminating CNs among the 11 possible classes (of Table 1). BMDP7M computed the weights, **W**, and constants, **c**, which constitute the linear discriminant function, d, for a feature vector, x, where $d_i(x) = x^t W_i + c_i$ [Duda and Hart, 1972]. Of the 23 computed features only 14 are required by the discriminant function, as determined by BMDP7M. The performance of the nodule expert, which characterizes the performance of ANDS, is summarized in the next section.

DISCUSSION

The three experts are based on appearance models: a local appearance model (rib); a global structural model (vascularity); and the physical properties of a nodule (nodule features). The performance of an expert depends on the accuracy of its model and the proficiency with which the model is translated into an algorithm. Thus, each descriptive model was obtained using the knowledge of an expert human; the rib and vascularity experts are solely based on my knowledge, while the nodule expert is based on appearance characteristics derived by observing radiologists. The image experts used these models in different ways, two of which were extensions of

the Hough transform. Because of the difficulty alone in qualitatively describing the difference between nodules and non-nodules, no nodule appearance model and relatively simple method (like those for ribs and vascularity) of detection could be devised. The appearance characteristics used by expert human nodule detectors were used instead in a traditional pattern recogniton system.

Performance of the rib expert may be improved by adding the following to the appearance model and updating the relational constraints for a non-rib: non-ribs contain nearly vertical parallel edges. Thus, a CN with nearly vertical parallel edges would be rejected as a rib.

The vascularity expert fails because it is based on an unsound model. Vascular structure is not straight and the CNs that arise because of it do not lie in a line. Close inspection of Fig. 2 (pre-expert image) may reveal this. Such a notion of co-linearity, however, may be useful in reasoning about CNs that lie on a rib, which is essentially a linear structure.

The success of the experts can be evaluated in two ways: by comparing the film false negative rate of ANDS with and without the experts; and by comparing the number of CNs that a radiologist must sift through before being confident of having inspected a CN that was reported by ANDS. ANDS was tested with and without the experts on 37 chest radiographs that contain at least one nodular abnormality. Two films with nodules were mis-diagnosed by the unexpert system and four were mis-diagnosed by the system that used the experts; the corresponding true positive rates are 92% and 86%. Although these rates are higher than those of radiologists, no statistically valid comparasion may yet be drawn. The total number of CNs that a radiologist must inspect (in order to be 99% confident of having inspected a detected nodule) drops from 12 to 4 as a result of using the image experts. Thus, the image experts reduce the number of points that a radiologist must inspect.

Performance of the nodule expert may presumably be improved by training with additional radiographs which contain nodules.

ACKNOWLEDGEMENTS

I would like to thank Dana Ballard and Chris Brown for the time and the invaluable advice that they so freely gave. Christie Chuang of the Department of Biostatistics helped this work stay the course of statistical validity. John Wandtke of the Department of Diagnostic Radiology provided the films with which the program was trained and tested.

REFERENCES

Ballard, D.H., "Model-directed detection of ribs in chest radiographs," *Proceedings, International Joint Conference on Pattern Recognition*, 907-910, 1978.

Ballard, D.H. and J. Sklansky, "Tumor detection in radiographs," *Computers in Biomedical Research*, **6**, 299-321, 1973.

Dixon, W.J. and M.B. Brown. *BMDP-79.* Berkeley, CA: U. California Press, 1979.

Duda, R.O. and P.E. Hart, "Use of the Hough transformation to detect lines and curves in pictures," *CACM*, **15:1**, 11-15, Jan. 1972.

Garland, H.L. "Studies on the accuracy of diagnostic procedures," *Am. J. Roent.*, **82:1**, 25-38, July 1959.

Lampeter, W., "Design, tuning, and performance evaluation of an automated pulmonary nodule detection system," TR 120, Computer Science Department, U. Rochester, Feb. 1983.

Revesz, G. and H.L. Kundel, "Psychophysical studies of detection errors in chest radiology," *Radiol.*, **123**, 559-562, June 1977.

Yerushalmy, Y. et. al., "Reliability of chest radiography diagnosis of pulmonary lesions," *Amer. J. Surg.*, **89**, 231-240, Jan. 1955.

END

FILMED

4-85

DTIC